MRL-R-811

AR-002-409

DEPARTMENT OF DEFENCE

DEFENCE SCIENCE AND TECHNOLOGY ORGANISATION

MATERIALS RESEARCH LABORATORIES

MELBOURNE, VICTORIA

REPORT

MRL-R-811

MODELLING PENETRATION BY SLENDER HIGH KINETIC ENERGY PROJECTILES

R.L. Woodward

Approved for Public Release

APRIL, 1981

DEPARTMENT OF DEFENCE

MATERIALS RESEARCH LABORATORIES

REPORT

MRL-R-811

MODELLING PENETRATION BY SLENDER HIGH KINETIC ENERGY PROJECTILES

R.L. Woodward

ABSTRACT

A model for the quantitative description of penetration by slender, high kinetic energy projectiles is presented and its usefulness assessed by comparison of computations with experimental data. The influence on behaviour of projectile shape and erosion effects are discussed and a parametric study is performed to indicate the strong influence of penetrator and target density and of target strength on depth of penetration into semi-infinite metal targets.

Approved for Public Release

POSTAL ADDRESS: Chief Superintendent, Materials Research Laboratories
P.O. Box 50, Ascot Vale, Victoria 3032, Australia

DOCUMENT CONTROL DATA SHEET

Security classification of this page: UNCLASSIFIED

1. *DOCUMENT NUMBERS:*
   a. *AR Number:* AR-002-409
   b. *Series & Number:* REPORT MRL-R-811
   c. *Report Number:* MRL-R-811

2. *SECURITY CLASSIFICATION:*
   a. *Complete document:* UNCLASSIFIED
   b. *Title in isolation:* UNCLASSIFIED
   c. *Abstract in isolation:* UNCLASSIFIED

3. *TITLE:*
MODELLING PENETRATION BY SLENDER HIGH KINETIC ENERGY PROJECTILES

4. *PERSONAL AUTHOR(S):*
WOODWARD, R.L.

5. *DOCUMENT DATE:* APRIL, 1981

6. *TYPE OF REPORT & PERIOD COVERED:*

7. *CORPORATE AUTHOR(S):*
Materials Research Laboratories

8. *REFERENCE NUMBERS:*
   a. *Task:* DST 77/069
   b. *Sponsoring Agency:*

9. *COST CODE:* 514820

10. *IMPRINT (Publishing establishment)*
Materials Research Laboratories,
P.O. Box 50, Ascot Vale, Vic. 3032
APRIL, 1981

11. *COMPUTER PROGRAMME(S): (Title(s) and language(s)):*
SLAM
FORTRAN IV

12. *RELEASE LIMITATIONS (of the document):*

Approved for Public Release

12-O. *OVERSEAS:* N.O. [ ] P.R. [1] A [ ] B [ ] C [ ] D [ ] E [ ]

13. *ANNOUNCEMENT LIMITATIONS (of the information on this page):*
No Limitation

14. *DESCRIPTORS:*
630 / Penetration // 636 / Kinetic energy projectiles //
645 / Rod penetrators : Mathematical models : Computer programs : Slam //

15. *COSATI CODES:* 1904

16. *ABSTRACT (if this is security classified, the announcement of this report will be similarly classified):*

A model for the quantitative description of penetration by slender, high kinetic energy projectiles is presented and its usefulness assessed by comparison of computations with experimental data. The influence on behaviour of projectile shape and erosion effects are discussed and a parametric study is performed to indicate the strong influence of penetrator and target density and of target strength on depth of penetration into semi-infinite metal targets.

CONTENTS

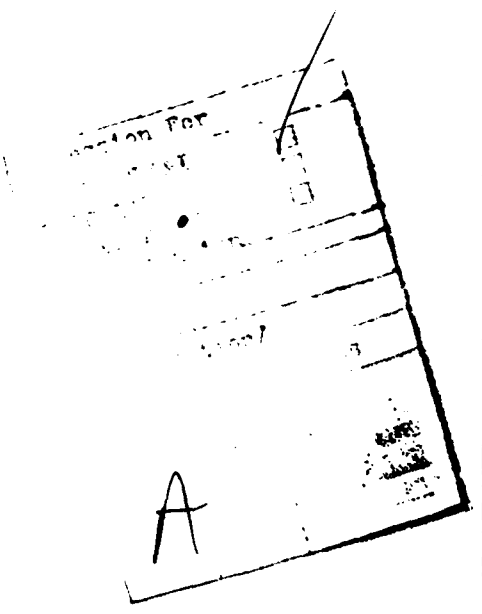

MODELLING PENETRATION BY SLENDER HIGH KINETIC ENERGY PROJECTILES

INTRODUCTION

Slender, high kinetic energy projectiles are formidable weapons for the defeat of armour and hence research into aspects of improvement of such projectiles and the armour for their defeat is a high priority task. Whilst engineering developments have been outstanding in this area, scientific investigations of the mechanics of penetration have been following rather than guiding the progress. Computer codes have been developed which can handle certain aspects of the problem in three dimensions, and which have had some success in studying penetration. However the codes cannot at this stage successfully treat deep penetrations and, in many of the problems which they do simulate successfully, the physics tends to be hidden by the complexity and detail of the output.

This report deals with an alternative approach to the quantitative description of deep penetration. In earlier work [1] a model was developed which transforms the problem of penetration by a deforming projectile into a one dimensional system. This model is described and comparisons of calculations using the model with a range of experimental data are presented both to assess the accuracy of the model and to investigate the influence of projectile shape on penetration behavior. A parametric study on the influence of material properties on the depth of penetration is performed, and the mechanics of projectile break-up and erosion are considered. The computer program for the model is listed in the Appendix with a sample input and output.

DESCRIPTION OF THE MODEL

The problem being considered is that of deep penetration of a semi-infinite target by a cylindrical rod projectile. The model is outlined below with a description of certain physical aspects and the principal equations; a more detailed discussion of the assumptions has been given elsewhere [1].

Figure 1 shows an idealized picture of a penetrator being fired into a semi-infinite target and the equivalent model of two cylinders impacting end on; one had an initial velocity equal to the projectile velocity and one was initially at rest. The model projectile and target cylinders are divided into a series of elements and the stress state of each element is considered individually. Target material experiences a constraint to radial motion due to the necessity to displace surrounding material; this effectively increases the flow stress and is taken into account by adding a constraint factor. Target elements also experience a shear stress along their edges as they are pushed forward in the target. Projectile elements within the target whose diameter is sufficient to touch the sides of the hole, defined as the diameter of the interface projectile element, also experience constraint to their deformation due to the surrounding target material and shearing at the edges between the projectile and the target. Other projectile elements experience no constraint or shearing. A further restriction on the radial motion comes from the influence of radial inertia, a term which is used to account for the work associated with acceleration of material in the radial direction as a cylindrical element is compressed at constant velocity.

To mathematically handle the problem each cylindrical element of penetrator and of target is represented by a point mass and a connecting link whose length equals the element length, the diameter of the cylinder being calculated from the length assuming constant volume deformation. The division of projectile and target into masses and ligaments is illustrated in Fig. 2. The method is based on a solution to the projectile mushrooming problem by Hashmi and Thompson [2] and the equations of motion of mass m_i at time t_j are given by

$$N_{i+1,j} - N_{i,j} - T_{i,j} - m_i \ddot{u}_{i,j} = 0 \qquad 1(a)$$

$$N_{i,j} - N_{i-1,j} + T_{i,j} - m_i \ddot{u}_{i,j} = 0 \qquad 1(b)$$

Equation 1(a) applies to the projectile and equation 1(b) applies to the target. The subscript notation is different for the penetrator and the target as the sequence of masses and ligaments is reversed at the interface as shown in Fig. 2.

N_i is the normal force on element i,

T_i the shear force,

$\ddot{u}_i$ the acceleration and

m_i is the element mass.

Having obtained the acceleration of the mass from equations (1), the new element positions (u_i) are obtained using the central difference equation [2]

$$u_{i,j+1} = \ddot{u}_{i,j} (\delta t)^2 + 2u_{i,j} - u_{i,j-1} \qquad (2)$$

and the time increment (δt) is related to the time (t_j) through

$$\delta t = t_{j+1} - t_j \tag{3}$$

The magnitude of the shear force (T_i) on an element of material is given by

$$|T_{i,j}| = \frac{\pi}{\sqrt{3}} D_{i,j} h_{i,j} \sigma_o^* \tag{4(a)}$$

and

$$|T_{i,j}| = \frac{\pi}{\sqrt{3}} D_{20,j} h_{i,j} \sigma_{ot} \tag{4(b)}$$

where 4(a) applies to a projectile element and 4(b) to a target element; the equations equate the shear force to the shear flow stress times the area of the cylindrical element surface. The material is assumed rigid/plastic in shear and the strength is related through the von Mises criterion to the strength σ_o of the material, described below. For the projectile the σ_o value chosen (σ_o^*) is the lesser of σ_{op} and σ_{ot} for the projectile and target respectively to represent shearing at the interface in the weaker solid. For the target σ_{ot} is used. D_i is the element diameter and h_i is the element height. For the target all elements are taken to have a diameter equal to the projectile interface diameter for the shear calculations to simulate a plug of this diameter being pushed forward in the target; for the program given in the appendix, this is element 20 and hence the use of D_{20} in equation 4(b). The sign of the shear force is set such that the shear force opposes the motion of the element. All target elements are subject to a shear force if they move; only those projectile elements which move and at the same time are below the target surface and have a diameter greater than or equal to the interface element diameter ($D_i \geq D_{20}$) experience a shear force. For these calculations we have had to define a target surface and a hole diameter; the target surface is the initial position of the interface as modified by the movement of the last element, which is generally negligible in the time of the event, and the hole diameter is defined as the diameter of the interface projectile element.

The normal force (N_i) on an element is given by

$$N_i = (\sigma_i + \sigma_{ri})(A_i + A_{i-1})/2 \tag{5(a)}$$

and

$$N_i = (\sigma_i + \sigma_{ri})(A_i + A_{i+1})/2 \tag{5(b)}$$

Equation 5(a) applies to the projectile and 5(b) to the target.

σ_i is the compressive flow stress of the material, a function of its strain,

σ_{ri} is an increment in stress due to radial inertia,

and A_i is the area of element i calculated by assuming deforming elements maintain a constant volume.

The use of a mean area in equations (5) has been justified by Woodward and Lambert [3] who demonstrated that it leads to a more accurate differencing scheme for the basic Hashmi and Thompson [2] method. The stress due to radial inertia is based on solutions for the axial compression of cylinders [4-6]. With a material of density ρ and considering each element as a cylinder with end velocities $\dot{u}_i$, the relation for σ_{ri} is

$$\sigma_{ri} = \frac{3}{64} \rho_p \left(\frac{D_i}{h_i}\right)^2 (\dot{u}_i - \dot{u}_{i-1})^2 \qquad 6(a)$$

and

$$\sigma_{ri} = \frac{3}{64} \rho_t \left(\frac{D_i}{h_i}\right)^2 (\dot{u}_{i+1} - \dot{u}_i)^2 \qquad 6(b)$$

where equation 6(a) applies to the projectile and 6(b) to the target.

Each material is characterized by a stress/strain relation of the form

$$\sigma = \sigma_o \varepsilon^n \qquad 7(a)$$

and an elastic modulus E which is used for unloading. σ_o and n are constants and ε is the strain. As noted previously, the material is assumed to be rigid/plastic in shear so that using the von Mises criterion the shear yield stress is taken as $\sigma_o/\sqrt{3}$. The shapes of the stress/strain curves used for various situations are illustrated in Fig. 3. For compression the target elements follow the relation

$$\sigma = 2.7\, \sigma_{ot}\, \varepsilon^{n_t} \qquad 7(b)$$

on loading and unload along an elastic line of constant slope. The factor 2.7 is the constraint factor included in the program to account for the restriction to radial flow due to the surrounding material in the target; it can be determined by independent quasi-static mechanical tests [7]. Projectile elements which are unconstrained use their uniaxial stress/strain relation as expressed in the form of equation 7(a); however if projectile elements are inside the target and have a diameter greater than the hole diameter they have a stress/strain relation of the form

$$\sigma = \sigma_{op}\, \varepsilon^{n_p} + 1.7\, \sigma_{ot} \qquad 7(c)$$

The contribution of target strength is for constraint.

All unloading uses an elastic line of equation

$$\sigma = \varepsilon E + c \qquad (8)$$

where the constant c is determined from the state of plastic strain at each step. As a simplification work hardening was only allowed after reloading past the previous maximum compressive strain; as very little unloading occurs this is not a severe penalty.

In the program a single parameter can be used to specify whether or not

constraint and shear stresses are to apply to projectile elements. This parameter, B_i, is specified as one if constraint and shear stresses apply to projectile elements and zero if they do not. At the surface of the target B_i is graded between zero and one, linearly, to give a smooth transition.

Erosion of an element has been allowed for if it is reduced to less than one tenth its original length; this is an arbitrary figure and was used to signify the effective removal of the mass from the zone of interest when its radial displacement became large. The significance of erosion mechanisms to projectile break-up is discussed later; however it is noted that for all cases of projectiles of practical dimensions considered in this report, erosion by radial flow of material, as allowed for in the model, did not occur.

The computer program is listed in the Appendix with a sample input and output and a description of some of the symbols and options. The program listed uses 20 projectile and 30 target elements. For the calculations reported in this work this program was only used if the length to diameter ratio of the projectile was greater than ten. For all other calculations a version with 10 projectile and 20 target elements was used; the difference in the calculations using the different element numbers is very small. The computer program treats one specific problem, the penetration of a semi-infinite target by a cylindrical projectile. A model of the mechanics has been built into the program as described above and the object is to use this model to enable quantitative calculations to be made which should give us an understanding of the penetration process. If the model gives useful insight and quantitative answers, then it should be possible to use the same basic approach with more complex problems.

COMPARISON WITH EXPERIMENT

The model was initially developed in comparison with small scale experiments and these results are given below. To test the model more thoroughly, comparison is also made with published experimental data for larger rounds, rounds of high length to diameter ratio, and cases in which the shape of the round significantly influences the results.

Plots of projectile final length and depth of penetration as a function of velocity are given in Fig. 4(a) for copper (A) cylinders fired into 2024 aluminium-alloy (B) targets, and in Fig. 4(b) for sintered tungsten alloy Kennertium W2 (C) cylinders fired into mild steel (D) targets. The letter designating each material allows its mechanical properties to be identified in Table I. Examination of Fig. 4 shows there is an underestimate of depth of penetration for the copper projectiles fired into aluminium; however, otherwise the quantitative agreement is quite good. The depth of penetration increases continuously with increasing velocity; however the projectile final length appears to approach a lower limit at the higher input velocities. This lower limit is associated with the restriction to radial expansion provided by the constraint of the surrounding target material and by the radial inertia. The strength parameters for these materials, listed in

Table I, were determined by uniaxial compression tests on the same materials as used in the ballistic experiments.

Tate et al. [8] published data for depth of penetration as a function of velocity for tungsten alloy rods fired into armour steel. The rods were of various weights up to 65 grams and for three length to diameter ratios, 3, 6 and 12; this represents a significantly larger scale than the previous case. The properties assumed for the tungsten and armour steel for the calculations are given as E and F respectively in Table I and are based on experimental data for what are considered similar materials. Calculations were performed for all the mass, length to diameter ratio and velocity ranges used by Tate et al. and three curves result which are compared with the experimental data in Fig. 5. For the length to diameter ratio of three there is good agreement between the calculations and the experiment; however for higher length to diameter ratios the model underestimates the depth of penetration. The discrepancy is not ascribed to the assumed stress/strain properties but, as will be discussed below, may be due to a combination of the neglect of thermal softening effects and the fact that a more suitable erosion method based on shearing is required. Nevertheless the general velocity dependence of the depth of penetration predicted by the model is correct.

Figure 6 gives plots of experimental data for flat tungsten cylinders and ogive tungsten and U - 2Mo alloy penetrators obtained by Brooks and Erickson [9]. The results demonstrate the significant influence that shape can have on performance at low velocities; above a certain transition velocity the curves for the ogive penetrators drop back close to the curve for flat-ended tungsten projectiles. As shape cannot be handled with the model, a comparison was made with the flat-ended case using σ_o and n values for the materials estimated from the Brooks and Erickson [9] data. For the tungsten, the properties are given as material G in Table I and the projectile mass used was 36.4 g, which is the same as the mass used in the experiments for both the cylinder and the ogive cases. For the target, material I in Table I, the σ_o and n values were forSAE 4130 steel of the same hardness as theSAE 4340 steel used in the experiments. Calculations were also performed for a flat-ended U - 2Mo alloy penetrator, material H in Table I, using a mass of 39.3 g which is the mass of the experimental ogive penetrators. The agreement of the model calculations, Fig. 6, with the experimental results for flat-ended penetrators is quite good. Furthermore, comparison of data above the transition velocity for ogive tungsten and U - 2Mo alloy rounds indicates that the latter penetrates deeper at the same velocity and this is indicated correctly by the model calculations for cylinders of the same mass, as used in the experiments.

Based on these comparisons between the model and experiments, it is clear that the general features of penetration depth and penetrator deformation as a function of length to diameter ratio and velocity can be handled for cylindrical projectiles; furthermore the quantitative results are useful. Care must be taken with calculations for penetrators which have significant deviations from a cylindrical shape as the model greatly underestimates their penetration efficiency at low velocities. At high velocities shape is not as important; however at these velocities the model tends to underestimate penetration depth. In developing the model the

influence of strain rate and thermal softening were ignored and all calculations use isothermal quasi-static stress/strain data. To a certain degree the thermal softening will be balanced by the increased flow stress due to the high strain rate; however it is suspected that thermal softening may be dominant at the highest speeds and lead to some departure of the model from experiment. It may be possible to include both strain-rate effects and thermal softening with a subroutine for situations in which sufficient materials data are available; however, in comparing materials, particularly if they are similar, some progress can be made by doing a comparative study with isothermal quasi-static data. Another way of improving the model would be to give consideration to other erosion mechanisms as will be discussed in the next section. The model itself is an approximation and an appreciation of its accuracy is more useful than complicating the physical description for the sake of coincidence with experiment at all points.

PROJECTILE EROSION AND BREAK-UP

The results of Brooks and Erickson [9] in Fig. 6 show a transition at high velocities where increase in projectile velocity leads to a reduction in depth of penetration; the transition is very material dependent and has been shown to be a function of projectile geometry [10]. A similar transition was observed with the present model calculations at high velocities, the transition being associated with the rapid erosion of elements in the form in which erosion is included in the model. In this section the phenomenon is examined, keeping in mind the simple concept of erosion which is being used.

In the model, as it presently stands, projectile elements are allowed to erode if their height is reduced to 0.1 of the original (diameter increased by a factor of $\sqrt{10}$). This factor is arbitrary and can be changed simply in the program; however, it is an expression of the fact that large-diameter elements would be eroded at their edges and the remaining mass would be insignificant compared with that of other elements and is thus removed from the calculation. With the practical problems considered in the previous section, erosion by the proposed mechanism did not occur with the factor set at 0.1; this is principally because the stress due to radial inertia becomes high for squat elements. The situation is more interesting, however, if the projectile diameter is made small.

Figure 7 shows some of Brooks [10] data replotted for tungsten projectiles (Kennertium W2) fired into SAE 4340 steel blocks. The penetrator was ogival but with a rounded nose of radius 1.27 mm (approximately 2.5 mm diameter). The transition shown in this figure is the smallest observed by Brooks [10]. It was absent for cylindrical projectiles of the same calibre, and it increased in magnitude as the tip diameter in the ogival projectiles was decreased. A plot of depth of penetration as a function of velocity calculated from the model for cylindrical projectiles of the same diameter (8.86 mm) and mass using properties of materials C and I in Table I is also given in Fig. 7 for comparison; as with the case of Fig. 6 the depth of penetration is underestimated partly due to the shape effect. An examination of the influence of projectile diameter on penetration behavior is made as

follows. Keeping projectile length and density constant, the radius, and hence the projectile mass also, was reduced and depth of penetration versus velocity curves plotted in Fig. 7. This was done for various projectile radii. There is a significant change in the shape of the depth/velocity curve between 2.0 mm and 1.5 mm diameter which is associated with the elimination of elements by the erosion mechanism and at 1.0 mm diameter a drop in depth with increased velocity occurs as elements are eroding continuously. For practical velocities ($< 2000\ ms^{-1}$) and these material properties, this mechanism of erosion occurs only for projectile diameters less than 2.0 mm diameter; the exact dimension depends on the figure selected for the height reduction at which an element is deleted and to this extent the discussion of the phenomenon is only semi-quantative.

The theoretical results can be summarized as follows. For large-diameter high-density projectiles, the radial inertia term is sufficient to prevent unrestricted radial flow of the projectile. Erosion of such projectiles must occur by other means which would include shearing off of the edges of elements which have expanded at the front of the projectile, for penetrators of limited ductility fracture of deformed elements, and in some cases perhaps adiabatic shear failures. For small-diameter projectiles, the radial inertia is too small to restrict the radial expansion and hence removal of material from the line of penetration by radial expansion, and effectively from the problem, is possible. For the present material properties, this erosion rate is significant if the projectile diameter is less than about 1.5 mm, depending on the criterion used to discard elements in the model.

The calculated projectile diameter at which erosion by this mechanism becomes significant is of the same order of magnitude as the projectile tip diameter at which the transition in behavior in Brooks' [9] results also becomes significant; furthermore, the velocity range is approximately correct. The following explanation in terms of the model is essentially that suggested by Brooks [10]. If the tip of the projectile is of small diameter, then at high velocities it can flatten rapidly by radial ejection of material. The projectile which is left is closer to a cylindrical shape and hence at high velocities the depth/velocity relation should be closer to that of a cylinder. Above a certain tip diameter, radial inertia prevents unrestrained collapse of the tip and hence no change in behavior is observed; instead, the geometry is such that the behavior can be expected to be closer to that of a cylinder over the whole velocity range.

The improved performance of ogive projectiles over flat-ended projectiles at low velocities, as illustrated by the results of Brooks and Erickson [9] in Fig. 6, indicates that at such velocities they are more resistant to deformation. In experiments using sintered-tungsten conically-ended projectiles fired into steel targets, the remarkable stability of the nose at low velocities was demonstrated [1] and such a case is shown in Fig. 8. The present model gives no clue to the stress situation in such penetrators which leads to increased stability and better performance at low velocities. On the other hand, the break-up of the tip leading to a more nearly flat-ended projectile at high velocities means that shape considerations are less important at high velocities and the model does have some application to these projectiles at high velocities.

As indicated above, erosion based on the simple concept used in the formulation of the model does not occur for cylindrical projectiles of practical diameter at typical ordnance velocities. Thus the severe deformation and mass reduction of such penetrators must be considered in other terms. In the calculations performed in cases where there was no erosion, Figs. 4, 5 and 6, reductions in projectile length by a factor of five were common; this represents slightly more than a doubling of the diameter but is a significant geometry change and a large amount of strain. It is to be expected that, with such large strains, materials of limited ductility may fracture; furthermore, significant heating of the projectile and target might lead to adiabatic shear instabilities if the thermomechanical properties of the materials are suitable. Fracture and adiabatic shear will only be important where there is a possibility of material breaking off from the line of penetration, and this is most likely at the edges of the penetrator and on breakout from finite thickness target plates. A further mechanism of material removal is by shearing at the sides of the penetrator. Although shearing of the edges is necessarily included in the model in the calculation of force equilibrium, indicating its importance, the shear displacements were not accounted for and with deep penetrations they would be expected to be large. The use of shearing as an erosion mechanism would probably be more realistic than the mechanism which is presently included in the model. This would permit a gradual reduction in the mass of each element and removal of material from the projectile in contrast to the present situation where no mass is removed for practical problems. The difficulty is to decide on an appropriate diameter at which shearing is to occur.

Whilst this discussion of projectile failure is largely qualitative it is felt that the model gives some indications of possible behavior. The breakdown of ogive penetrators at high velocities can be explained in terms of flattening of the tip by unrestrained radial expansion, as was suggested by Brooks [10]. At practical velocities and projectile geometries, erosion by such a mechanism is not generally applicable to rod-shaped projectiles and we must look at other mechanisms such as the large plastic strains, fracture, adiabatic shearing and plastic shearing at the projectile/target interface to explain shape changes and mass losses for such rounds.

PARAMETRIC INVESTIGATION

The principal material parameters considered in the model which may effect performance of a penetrator or target are the density (ρ), strength (σ_o), and work hardening exponent (n). Using a particular case for the results of Tate et al. [7], these parameters were increased and decreased, generally by ten percent, to see how much they would alter the depth of penetration into the semi-infinite target. The basic case considered was for a projectile of length to diameter ratio 3, mass 33.7 g and diameter 9.45 mm travelling at 1500 ms^{-1}. The input for this situation is used as the example problem in the Appendix. Each material parameter was varied in turn by ten percent and the results compared with the basic run. One limitation to the following discussion, therefore, is that it is centred around a particular set of conditions.

Ten percent variations in the work hardening exponent (n) of the projectile and the target gave less than one percent change in depth of penetration. Surprisingly, the effect of penetrator strength (σ_{op}) was also negligible. Because of the significance of this result, the penetrator strength was permitted to cover a wider range from the standard value of 932 MPa and, as shown in Fig. 9, there is negligible influence on depth of penetration over a wide range. An explanation of this may be that the stresses due to the constraint of the target and the radial inertia may be much greater than the penetrator flow stress. On the other hand an increase in target strength (σ_{ot}) of ten percent gave approximately six percent reduction in depth of penetration; these calculations were also extended over a wider range from the initial 1269 MPa and the results are shown in Fig. 9.

A ten percent increase in penetrator density, and hence an equivalent increase in mass and kinetic energy for the same size and velocity penetrator, gave approximately eight percent increase in depth of penetration. A ten percent reduction in target density gave slightly less than one percent increase in depth of penetration; however, in terms of areal density, this represents a reduction of approximately ten percent for a material of the same strength. Whilst changes in density of the target by such figures are only of academic interest for a particular material, they do indicate possible benefits by changing the material itself to obtain a lower density.

Of the parameters considered, only target strength and density and penetrator density gave significant changes in performance. A parameter not included in the model, which is undoubtedly important, is ductility. As penetrator strength is not critical it becomes clear that sacrificing strength for increased ductility is a possibility. The model does not account for the influence which strength may have in providing stiffness to resist buckling on oblique impact and deformation during launch.

CONCLUSION

A model for the deep penetration of semi-infinite metal targets by cylindrical projectiles has been described and quantitative calculations compared with published experimental data. The model was used to examine materials parameters which influence performance of projectiles and armour. Density of the target and the penetrator and target strength are shown to have large influences on penetration depth in normal impacts. The principal aspects which the model does not consider are oblique impact and penetrator ductility.

REFERENCES

1. Woodward, R.L. "Penetration of Semi-Infinite Metal Targets by Deforming Projectiles". Accepted for Publication in Int. Jnl. Mech. Sci.

2. Hashmi, M.S.J. and Thompson, P.J. (1977). "A Numerical Method of Analysis for the Mushrooming of Flat-Ended Projectiles Impinging on a Flat Rigid Anvil". Int. Jnl. of Mech. Sci. 19, 273.

3. Woodward, R.L. and Lambert, J.P. "A Discussion of the Calculation of Forces in the One Dimensional Finite Difference Model of Hashmi and Thompson". Accepted for Publication in Int. Jnl. Mech. Sci.

4. Dharan, C.K.H. and Hauser, F.E. (1970). "Determination of Stress-Strain Characteristics at Very High Strain Rates". Experimental Mechanics 10, 370.

5. Sturgess, C.E.N. and Jones, M.G. (1971). "Estimation of Dynamic Forces in High-Speed Compression using a Free-Flight Impact Forging Device". Int. Jnl. of Mech. Sci. 13, 309.

6. Johnson, W. (1972). "Impact Strength of Materials", Arnold, 152.

7. Woodward, R.L. and de Morton, M.E. (1976). "Penetration of Targets by Flat-Ended Projectiles". Inst. Jnl. of Mech. Sci. 18, 119.

8. Tate, A., Green, K.E.B., Chamberlain, P.G. and Baker, R.G. (1978). "Model Scale Experiments on Long Rod Penetration". Fourth Int. Symp. on Ballistics, Monterey, Calif., ADPA.

9. Brooks, P.N. and Erickson, W.N. (1971). "Ballistic Evaluation of Materials for Armour Penetrators", Defence Research Establishment Valcartier, Canada, DREV R-643/71.

10. Brooks, P.N. (1974). "Ballistic Impact - the Dependence of the Hydrodynamic Transition Velocity on Projectile Tip Geometry". Defence Research Establishment Valcartier, Canada, DREV R-4001/74.

APPENDIX

A description is given of certain particular aspects of the program that is used for the computations (SLAM) followed by a listing of the program and a typical input and output. The program uses twenty elements for the projectile and thirty elements for the target, which has been more than sufficient for most problems. Care must be exercised if it is necessary to change the element numbers or the equations of the program as some fixed constants throughout the program are based on the element numbers and also it is necessary to trace the units from the input. Sufficient comment statements have been added to identify various sections and the logic should be traceable using the equations set out in this report.

Input parameters which are easily determined are projectile mass, velocity and diameter and projectile and target densities and Young's Moduli. The materials parameters σ_o and n are obtained by fitting material stress/strain data to equation 7(a) using a log/log plot for both the penetrator and target materials. In doing this, better results should be obtained by using compressive data with a loading axis coinciding with the expected impact direction for both penetrator and target in order to account for the influence of texture effects on strength. Furthermore, as it is a high strain problem, the curve fitting of the stress/strain data is more appropriately done using the high strain data. The choice of target thickness for input to the model should be made so that each of the thirty elements is not excessively large, at the same time too thin a target which results in the rear elements being noticeably deformed should be avoided. If the target is too thin then the last element will indicate a significant velocity in the output and the calculation should be repeated with a thicker target. As a first guess, making the target thickness 1.5 to 2 times the projectile length is generally satisfactory. The maximum allowable time increment can be estimated as $\ell/200\sqrt{\rho/E}$ for twenty projectile elements where ℓ is the projectile length and ρ and E its density and Young's Modulus respectively. This is the elastic wave transit time for the minimum element length.

The principal output lists a number of parameters of general interest. MIN and MAX are the numbers of the end projectile and target elements respectively, furthest from the impact interface. If MIN is greater than 1 then projectile erosion has occurred and if MAX is less than 50 target erosion has occurred; each element removed changes these by one unit. The interface projectile element is 20 and the corresponding target element is 21. The diameters D(N) and Velocities W(N) of these interface elements and adjacent elements are printed. Furthermore the velocities of the end projectile, W(MIN), and target, W(MAX), elements are given. When the rear of the projectile is moving at less than 10 ms^{-1} or if all projectile elements have eroded then the problem is stopped. W(MAX) can be used to indicate if the rear of the target has picked up any significant velocity, which would indicate too thin a target to assume it to be semi-infinite. Length dimensions are in millimetres and velocities in kilometres per second in the output. The other important parameters in this output are the projectile height (HP), the depth of penetration (DP) and the time (T) in microseconds. Allowance has been made for the output of several other parameters for each element, however, the format statements may have to be changed to suit the particular problem.

```
      PROGRAM SLAM(TAPE1,TAPE2,TAPE3,TAPE4,TAPE5,TAPE6,TAPE7,TAPE8)
C
C     SLAM
C     CALCULATES DEPTH OF PENETRATION AND AMOUNT OF EROSION
C     FOR PENETRATORS ENTERING SEMI-INFINITE TARGETS
C     WRITTEN BY RAY WOODWARD   1979
C     MATERIALS RESEARCH LABORATORIES  MARIBYRNONG AUSTRALIA
C
      DIMENSIONP(71),U(71),UP(71),UD(71),UN(71),E(71),A(71),DS(71)
     2,S(71),D(71),W(71),ASS(71),B(71),DEP(71),TOR(71),DSL(71)
     4,C(71),DSP(71),SM(71),SMC(71)
   21 FORMAT(F5.3/F6.3/F6.1/F5.3/F6.2/F5.3/F5.2/F7.0/F7.0
     3/F5.2/F5.3/F6.1/F6.2)
   23 FORMAT(20F4.1/20F4.1/10F4.1)
   24 FORMAT(F3.0,18F7.0/18F7.0/12F7.0,F3.0)
   25 FORMAT(20F6.3/20F6.3/10F6.3)
   26 FORMAT(20F5.1/20F5.1/10F5.1)
   27 FORMAT(F3.0,18F6.0/18F6.0/12F6.0,F3.0)
   28 FORMAT(20F6.3/20F6.3/10F6.3)
   29 FORMAT(3F8.3,I3,8F8.3,I3)
   77 FORMAT(T3,'HP'T11,'DP'T20,'T'T24,'MIN'T29,'W(MIN)'T38,'W(19)'
     1T46,'D(19)'T54,'W(20)'T62,'D(20)'T70,'D(21)'T78,'W(22)'T85,'W(MAX)
     2'T91,'MAX')
      WRITE(8,77)
C     INPUT-DT  TIME INCREMENT  MICROSECS
C          -ASSP  MASS PROJ  GMS
C          -SOP  SIGMA ZERO PROJ  MPA
C          -ENP  WORK HARDENING INDEX  PROJ
C          -DO  DIAM PROJ MM
C          -V  VEL PROJ  KM/SEC
C          -ROP  DENSITY PROJ  GM/CC
C          -YP  YOUNGS MOD PROJ  MPA
C          -YT  YOUNGS MOD TARGET  MPA
C          -ROT  DENSITY TARGET  GM/CC
C          -ENT  WORK HARDENING INDEX  TARGET
C          -SOT  SIGMA ZERO TARGET  MPA
C          -DST  THICKNESS TARGET MM
      READ(1,21)DT,ASSP,SOP,ENP,DO,V,ROP,YP,YT,ROT,ENT,SOT,DST
      T=0
      DT2=DT**2
      ASST=.0007854*DST*ROT*(DO**2)
      ASPL=ASSP*.05
      ASTL=ASST/30
      AO=.7845*(DO**2)
      DSOP=(ASPL/(ROP*AO))*1E3
      DSOT=DST/30
      VDT=V*DT
      IF(SOP.GT.SOT)GO TO 34
      SOL=SOP
      GO TO 35
   34 SOL=SOT
C
C     37 SETS UP INITIAL PROJECTILE PARAMETERS
C
   35 DO37I=1,20
      P(I)=0
      U(I)=DSOP*FLOAT(I)
```

```
      UP(I)=U(I)-VDT
      UD(I)=0
      DSP(I)=DSOP
      DS(I)=DSOP
      E(I)=0
      A(I)=AO
      S(I)=0
      ASS(I)=ASPL
      B(I)=0
      TOR(I)=0
      DSL(I)=DSOP
      C(I)=0
      SM(I)=0
      SMC(I)=0
   37 CONTINUE
C
C     DPMIN-  MIN HEIGHT OF PROJ ELEMENT FOR EROSION
      DPMIN=DSOP/10.
C
C     38 SETS UP INITIAL TARGET PARAMETERS
C
      DO38I=2,30
      J=I-1
      N=I+20
      P(N)=0
      U(N)=U(20)+DSOT*FLOAT(J)
      UP(N)=U(N)
      UD(N)=0
      DSP(N)=DSOT
      DS(N)=DSOT
      E(N)=0
      A(N)=AO
      S(N)=0
      ASS(N)=ASTL
      TOR(N)=0
      DSL(N)=DSOT
      C(N)=0
      SM(N)=0
      SMC(N)=0
   38 CONTINUE
      UR=U(20)
C
C     DTMIN-  MIN HEIGHT OF TARGET ELEMENT FOR EROSION
      DTMIN=DSOT/10.
C
C     SET UP PARAMETERS FOR INTERFACE ELEMENT
      ASS(20)=ASTL+ASPL
      UP(20)=U(20)-SQRT(DT2*ASPL*(V**2)/ASS(20))
      W(50)=0
      DSL(21)=DSOT
      P(21)=0
      U(21)=U(20)
      UP(21)=UP(20)
      DSP(21)=DSOT
      A(21)=AO
      S(21)=0
      TOR(21)=0
```

```
C
C       LABEL FIRST,SECOND,LAST AND SECOND LAST ELEMENTS
        MIN=1
        MINA=2
        MAX=50
        MAXB=49
C
C       72 IS MAIN CALCULATION LOOP
C
        DO72K=1,50000
C
C       CALCULATE POSITION OF SURFACE OF TARGET
        UR=UR+W(MAX)*DT
C
C       CALCULATION OF MOVEMENT OF INTERFACE ELEMENT
        UD(20)=(P(21)-P(20)+TOR(21)+TOR(20))/ASS(20)*1E-6
        UN(20)=UD(20)*DT2+2*U(20)-UP(20)
        UP(20)=U(20)
        U(20)=UN(20)
        IF(MIN.GT.19)GO TO 391
C
C       39 CALCULATES MOVEMENT OF PROJ ELEMENTS
        DO39N=MIN,19
        M=N+1
        UD(N)=((P(M)-P(N)+TOR(N))/ASS(N))*1E-6
        UN(N)=UD(N)*DT2+2*U(N)-UP(N)
        UP(N)=U(N)
        U(N)=UN(N)
   39 CONTINUE
C
C       40 CALCULATES MOVEMENT OF TARGET ELEMENTS
 391    DO40N=22,MAX
        M=N-1
        UD(N)=((P(N)-P(M)+TOR(N))/ASS(N))*1E-6
        UN(N)=UD(N)*DT2+2*U(N)-UP(N)
        UP(N)=U(N)
        U(N)=UN(N)
   40 CONTINUE
        U(21)=U(20)
        UP(21)=UP(20)
C
C       43 CALCULATES NEW HEIGHTS OF PROJ ELEMENTS
        DO43J=MINA,20
        N=J-1
        DS(J)=U(J)-U(N)
        IF(DS(J).GT.DSL(J))GOTO 43
        DSL(J)=DS(J)
   43 CONTINUE
C
C       44 CALCULATES NEW HEIGHTS OF TARGET ELEMENTS
        DO44J=21,MAXB
        N=J+1
        DS(J)=U(N)-U(J)
        IF(DS(J).GT.DSL(J))GO TO 44
        DSL(J)=DS(J)
   44 CONTINUE
        DS(MIN)=DSOP
```

```
      DS(MAX)=DSOT
C
C     46 CALCULATES STRAIN AND STRESS IN PROJ ELEMENTS
C
      DO46J=MIN,20
      E(J)=ALOG(DSOP/DS(J))
      A(J)=A(J)*DSP(J)/DS(J)
      IF(DS(J).GT.DSL(J))GO TO 62
      S(J)=0.-SOP*(E(J)**ENP)-1.7*B(J)*SOT
      SM(J)=SOP*(E(J)**ENP)
      SMC(J)=S(J)
      C(J)=S(J)+YP*E(J)
      GO TO 54
   62 S(J)=-YP*E(J)+C(J)
      IF(S(J).LT.SM(J))GO TO 548
      S(J)=SM(J)
      C(J)=S(J)+YP*E(J)
      GO TO 54
  548 IF(S(J).GT.SMC(J))GO TO 54
      S(J)=SMC(J)
      C(J)=S(J)+YP*E(J)
   54 D(J)=1.12838*SQRT(A(J))
      DSP(J)=DS(J)
      IF(U(J).LE.UP(J))GO TO 32
      TOR(J)=-1.8137*D(J)*DS(J)*SOL*B(J)
      GO TO 31
   32 IF(U(J).LT.UP(J))GO TO 33
      TOR(J)=0
      GO TO 31
   33 TOR(J)=1.8137*D(J)*DS(J)*SOL*B(J)
   31 W(J)=(U(J)-UP(J))/DT
   46 CONTINUE
      P(MIN)=S(MIN)*A(MIN)
C
C     11 CALCULATES FORCE IN PROJ ELEMENTS
      DO11J=MINA,20
      JM=J-1
      IF(W(J).LT.W(JM))GO TO 111
      RIN=0
      GO TO 112
  111 RIN=-46.875*ROP*((W(J)-W(JM))*D(J)/DS(J))**2
  112 P(J)=(S(J)+RIN)*(A(JM)+A(J))/2
   11 CONTINUE
C
C     59 ASKS IF ANY ELEMENTS OF PROJ ERODED
C        IF SO 61 REZONES OTHERS
C
      DO59J=MINA,20
      IF(DS(J).GT.DPMIN)GO TO 59
      ML=J
      GO TO 58
   59 CONTINUE
      GO TO 56
   58 MIN=MIN+1
      MINA=MINA+1
      DO61N=MIN,ML
      J=ML+MIN-N
```

```
      JJ=J-1
      P(J)=P(JJ)
      U(J)=U(JJ)
      UP(J)=UP(JJ)
      DSP(J)=DSP(JJ)
      DS(J)=DS(JJ)
      E(J)=E(JJ)
      A(J)=A(JJ)
      S(J)=S(JJ)
      C(J)=C(JJ)
      DSL(J)=DSL(JJ)
      SM(J)=SM(JJ)
      SMC(J)=SMC(JJ)
      TOR(J)=TOR(JJ)
   61 CONTINUE
      IF(ML.LT.20)GO TO 56
      UP(20)=U(20)-SQRT(DT2*(ASPL*W(19)**2+ASTL*W(20)**2)/(ASTL+ASPL))
C
C     21 CALCULATES STRAIN AND STRESS IN TARGET ELEMENTS
C
   56 DO47J=21,MAX
      E(J)=ALOG(DSOT/DS(J))
      A(J)=A(J)*DSP(J)/DS(J)
      IF(DS(J).GT.DSL(J))GO TO 66
      S(J)=0.-2.7*SOT*(E(J)**ENT)
      SM(J)=0.-S(J)
      SMC(J)=S(J)
      C(J)=S(J)+YT*E(J)
      GO TO 18
   66 S(J)=-YT*E(J)+C(J)
      IF(S(J).LT.SM(J))GO TO 188
      S(J)=SM(J)
      C(J)=S(J)+YT*E(J)
      GO TO 18
  188 IF(S(J).GT.SMC(J))GO TO 18
      S(J)=SMC(J)
      C(J)=S(J)+YT*E(J)
   18 D(J)=1.12838*SQRT(A(J))
      DSP(J)=DS(J)
      IF(U(J).LE.UP(J))GO TO 48
      TOR(J)=-1.8137*D(20)*DS(J)*SOT
      GO TO 49
   48 IF(U(J).LT.UP(J))GO TO 488
      TOR(J)=0
      GO TO 49
  488 TOR(J)=1.8137*D(20)*DS(J)*SOT
   49 W(J)=(U(J)-UP(J))/DT
   47 CONTINUE
   19 P(MAX)=S(MAX)*A(MAX)
C
C     12 CALCULATES FORCE IN TARGET ELEMENTS
      DO12J=21,MAXB
      JM=J+1
      IF(W(J).GT.W(JM))GO TO 121
      RIN=0
      GO TO 122
  121 RIN=-46.875*ROP*((W(J)-W(JM))*D(J)/DS(J))**2
```

```
  122 P(J)=(S(J)+RIN)*(A(JM)+A(J))/2
   12 CONTINUE
C
C      ASK IF ANY ELEMENTS OF TARGET ERODED
C          IF SO 64 REZONES OTHERS
C
       IF(DS(21).GT.DTMIN)GO TO 51
       MAX=MAX-1
       MAXB=MAXB-1
       DO64N=21,MAX
       JJ=N+1
       P(N)=P(JJ)
       U(N)=U(JJ)
       UP(N)=UP(JJ)
       DSP(N)=DSP(JJ)
       DS(N)=DS(JJ)
       E(N)=E(JJ)
       A(N)=A(JJ)
       S(N)=S(JJ)
       ASS(N)=ASS(JJ)
       TOR(N)=TOR(JJ)
       C(N)=C(JJ)
       DSL(N)=DSL(JJ)
       SM(N)=SM(JJ)
       SMC(N)=SMC(JJ)
    64 CONTINUE
       UP(20)=U(20)-SQRT(DT2*(ASPL*W(20)**2+ASTL*W(22)**2)/(ASTL+ASPL))
       U(21)=U(20)
       UP(21)=UP(20)
    51 T=T+DT
C
C      67 DETERMINES WHICH PROJ ELEMENTS ARE INSIDE TARGET
C         WHICH HAVE DIAM .GT. INTERFACE DIAM---FOR USE IN
C         FRICTION AND CONSTRAINT CALCULATIONS VIA THE
C         PARAMETER B(N)
C
       DO67N=MIN,20
       DEP(N)=U(N)-DS(N)-UR
       IF(DEP(N).LT.0)GO TO 68
       B(N)=1
       GO TO 677
    68 DEP(N)=0.-DEP(N)
       IF(DEP(N).LT.DS(N))GO TO 69
       B(N)=0
       GO TO 67
    69 B(N)=(DS(N)-DEP(N))/DS(N)
   677 IF(D(N).GE.D(20))GO TO 67
       B(N)=0
    67 CONTINUE
       HP=0
C
C      81 AND 82 CALCULATE HEIGHT OF PROJ AND DEPTH OF PENETRATION
C
       DO81NZ=MIN,20
       HP=HP+DS(NZ)
    81 CONTINUE
       HT=0
```

```
      DO82NZ=21,MAX
      HT=HT+DS(NZ)
   82 CONTINUE
      DP=DST-HT
C
C     PRINTING
C
      DO83N=1,100
      INC=N*500
      IF(W(MIN).LE..01)GO TO 79
      IF(MIN.GT.19)GO TO 79
      IF(K-INC)72,79,83
   83 CONTINUE
C
C     79/2 TO 7 PRINT--POSITION,FORCE,HT,DIAM,STRESS AND VELOCITY
C
   79 WRITE(2,23)(U(I),I=1,50)
      WRITE(3,24)(P(I),I=1,50)
      WRITE(4,25)(DS(I),I=1,50)
      WRITE(5,26)(D(I),I=1,50)
      WRITE(6,27)(S(I),I=1,50)
      WRITE(7,28)(W(I),I=1,50)
C
C     179 PRINTS VARIETY OF PRINCIPLE PARAMETERS
  179 WRITE(8,29)HP,DP,T,MIN,W(MIN),W(19),D(19),W(20),D(20),D(21)
     1,W(22),W(MAX),MAX
      IF(W(MIN).LE..01)GO TO 99
      IF(MIN.GT.19)GO TO 99
   72 CONTINUE
   99 STOP
      END
```

TYPICAL INPUT

Quantity	Units	Meaning	Symbol in Program
.02	microseconds	time increment	DT
33.7	gm	penetrator mass	ASSP
932.	MPa	penetrator strength (σ_o)	SOP
.07	(dimensionless)	penetrator workhardening exponent (n)	ENP
9.45	mm	penetrator diameter	DO
1.5	km s^{-1}	penetrator velocity	V
17.0	gm cm^{-3}	penetrator density	ROP
272000.	MPa	penetrator Young's Modulus	YP
206841.	MPa	target Young's Modulus	YT
7.8	gm cm^{-3}	target density	ROT
.14	(dimensionless)	target workhardening exponent (n)	ENT
1267.	MPa	target strength (σ_o)	SOT
100.	mm	target thickness	DST

TYPICAL OUTPUT

HP	DP	T	MIN	W(MIN)	W(19)	D(19)	W(20)	D(20)	D(21)	W(22)	W(MAX)	MAX
21.807	8.623	10.000	1	1.480	.773	17.161	.752	17.160	17.191	.721	.001	50
14.267	15.530	20.000	1	1.441	.684	19.800	.679	19.772	18.454	.671	-.000	50
8.163	22.032	30.000	1	.781	.611	20.341	.609	20.366	18.753	.608	-.001	50
7.936	27.102	40.000	1	.408	.404	20.347	.404	20.329	18.717	.402	-.001	50
7.943	30.138	50.000	1	.209	.208	20.336	.208	20.317	18.701	.206	.001	50
7.939	31.257	60.000	1	.023	.019	20.340	.019	20.321	18.703	.017	.001	50
7.937	31.263	60.460	1	.010	.009	20.340	.009	20.320	18.701	.012	.001	50

TABLE I

MATERIALS PROPERTIES

Designation	Material Description	Strength σ_o(MPa)	Work Hardening Exponent, n	Density ρ(gm cm^{-3})	Function
A	Copper	443.	0.1	8.96	penetrator
B	2024T351 Aluminium	776.	0.096	2.7	target
C	Tungsten Alloy Kennertium W2	1967.	0.25	18.6	penetrator
D	Mild Steel	816.	0.19	7.8	target
E	Tungsten Alloy	932.	0.07	17.0	penetrator
F	Armour Steel	1267.	0.14	7.8	target
G	Tungsten Alloy	1146.	0.065	17.36	penetrator
H	U-2Mo Alloy	1268.	0.061	18.7	penetrator
I	SAE 4130 Steel	1290.	0.095	7.8	target

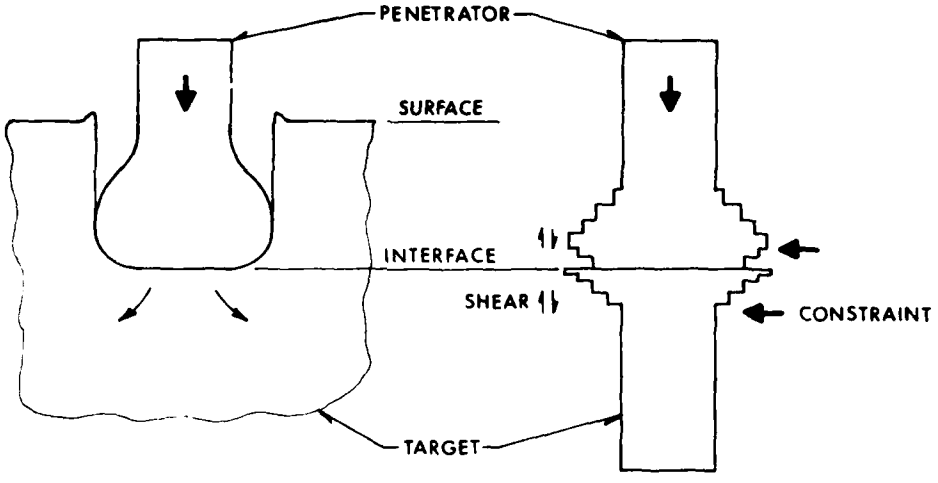

FIGURE 1 Schematic illustration of the correspondence between the geometry of penetration and the model using impacting cylinders. The distinction between penetrator and target cylinders is via the constraint which is experienced by all target elements but is selectively applied to projectile elements as discussed in the text.

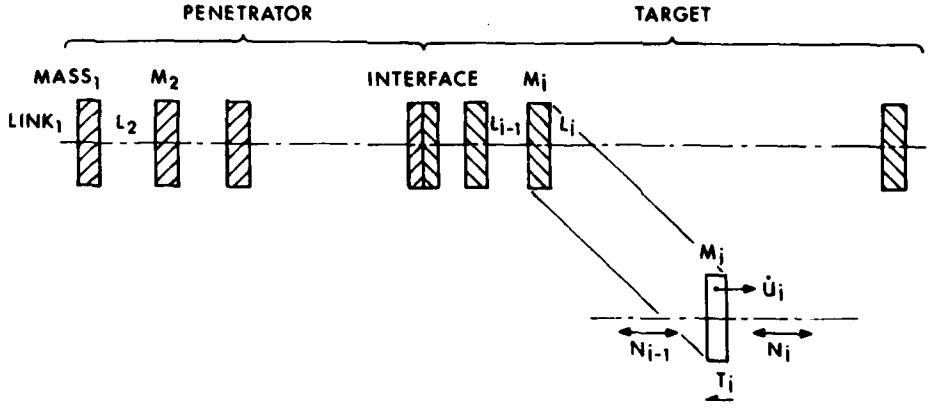

FIGURE 2 The division of the projectile and target cylinders into segments each consisting of a point mass, m_i and a massless link, L_i. The element at position u_i is moving at velocity $\dot{u}_i$ and is subject to normal forces, N_i, transmitted throughout links and shear forces, T_i, applied at the edge of each cylindrical element.

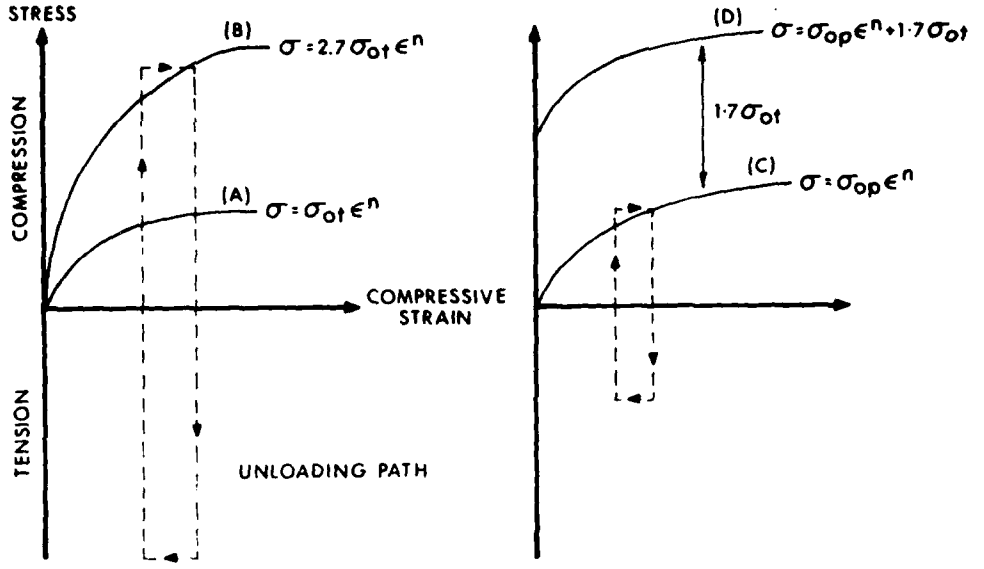

FIGURE 3 Stress/strain relations used for the target and the penetrator. Curve (B) is the form of the stress/strain curve for the target material obtained from uniaxial tension or compression tests. The model increases the strength to 2.7 times this value to obtain curve (A) which then includes the constraint and is the loading curve used for all target elements. The unloading path from (A) uses the target material Young's Modulus and work hardening is only allowed on further compressive loading to higher strain, an approximation. Curve (C) is the stress/strain properties obtained from uniaxial tension or compression tests on penetrator material and is used for unconstrained projectile elements and for unloading using the projectile Young's Modulus. Those projectile elements which are constrained are loaded along curve (D) which includes an increment due to the target constraint. Compressive stress and strain are plotted as positive in the diagram for convenience as loading occurs in compression and unloading is tensile in the problem.

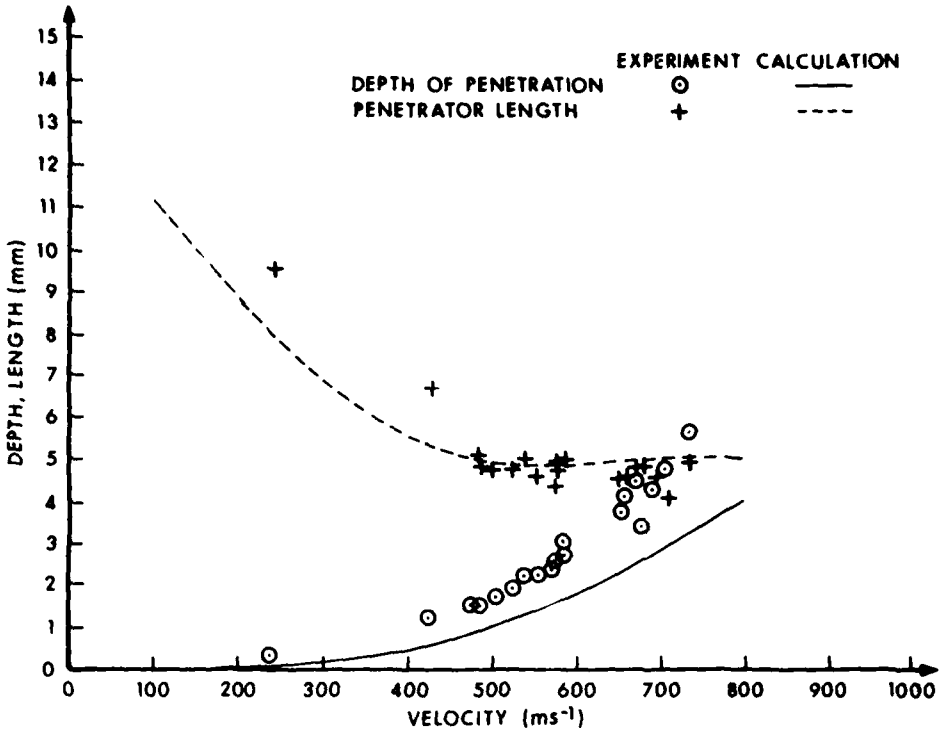

(a)

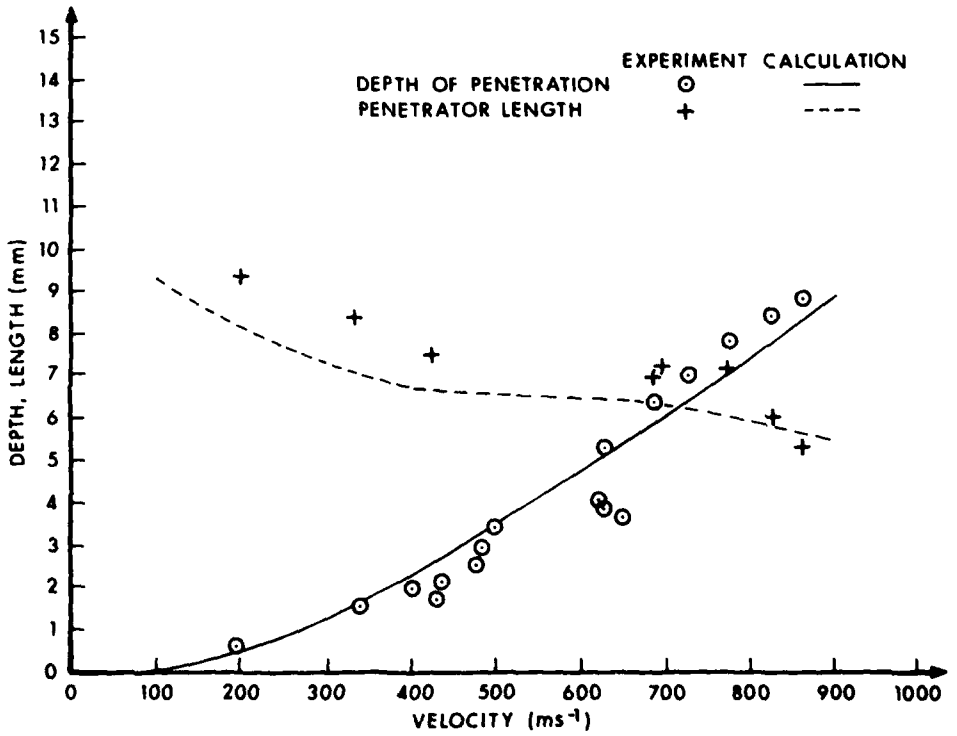

(b)

FIGURE 4 Comparison of depth of penetration and final penetrator length between experiment and model calculations for (a) 1.96 g copper cylinders of diameter 4.76 mm fired into semi-infinite 2024 T351 aluminium targets and (b) 3.29 g tungsten alloy, Kennertium W2, cylinders of diameter 4.76 fired into semi-infinite mild steel targets.

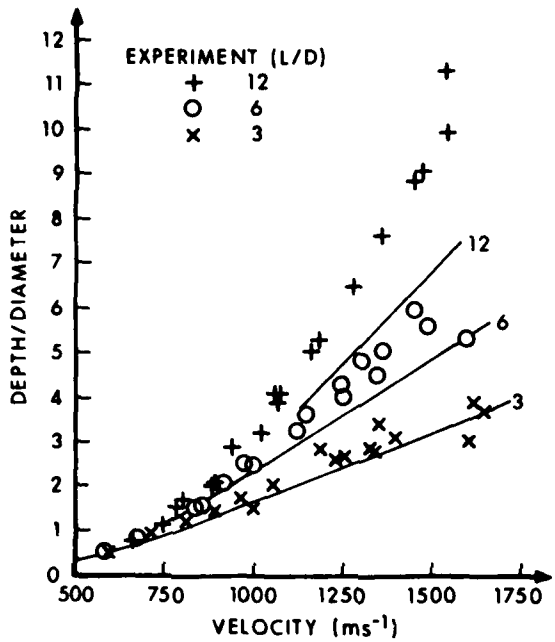

FIGURE 5 Depth of penetration divided by diameter plotted as a function of velocity for penetrators of three length to diameters (L/D) ratios. The experimental points were replotted from the work of Tate et al. [7]. The calculations with the model used the properties for materials E and F in Table I and covered all the mass and diameter ranges used by Tate et al. [7] resulting in three basic curves shown for the three L/D ratios.

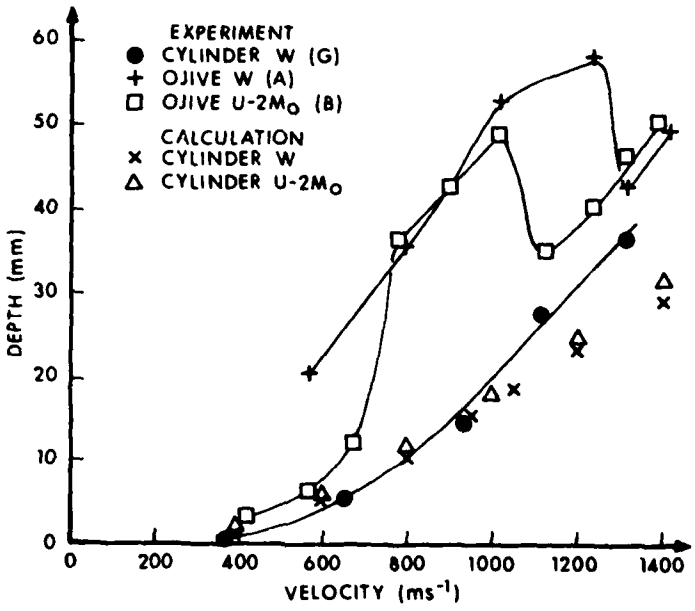

FIGURE 6 Plots of experimental results of Brooks and Erickson [8] for three cases, including cylinder and ogive projectiles of both tungsten and U-2Mo alloy materials; the letters G, A and B relate to the cases in the report of Brooks and Erickson [8] which were taken. Some calculations for cylindrical projectiles of the same mass and diameter are given for tungsten and U-2Mo alloys using the properties of materials G, H and I in Table I.

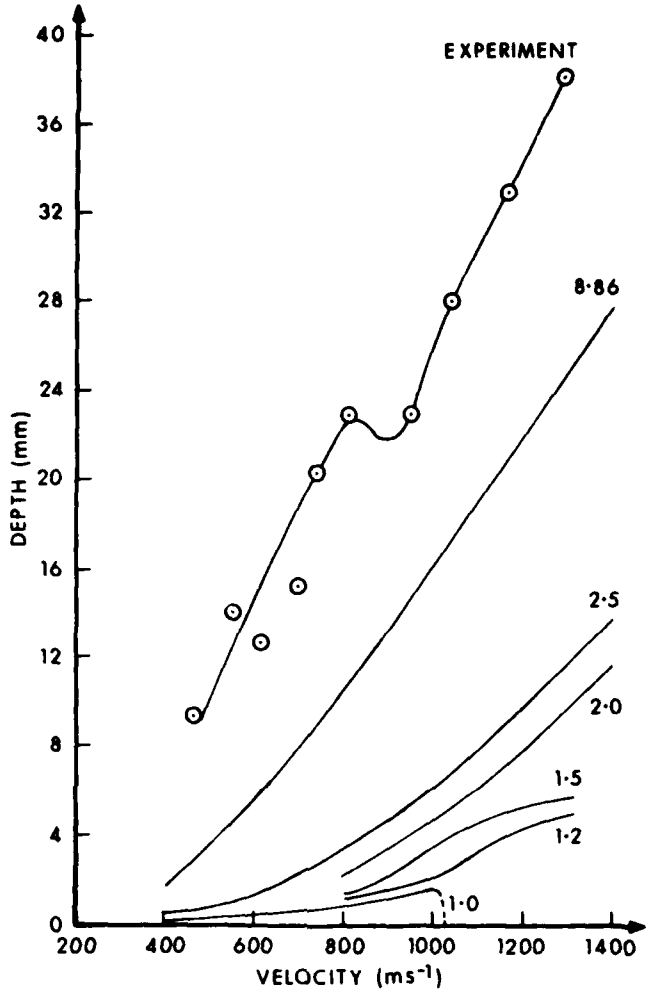

FIGURE 7 Plots of depth of penetration against velocity using the experimental data of Brooks [9] for tungsten alloy ogive projectiles with a 1.27 mm radius rounded nose and for calculations using material properties C and I in Table I. The calculations are for cylindrical projectiles of the same diameter (8.86 mm) and mass as the penetrator used by Brooks [9] and for smaller diameters, and mass, as indicated on the curves.

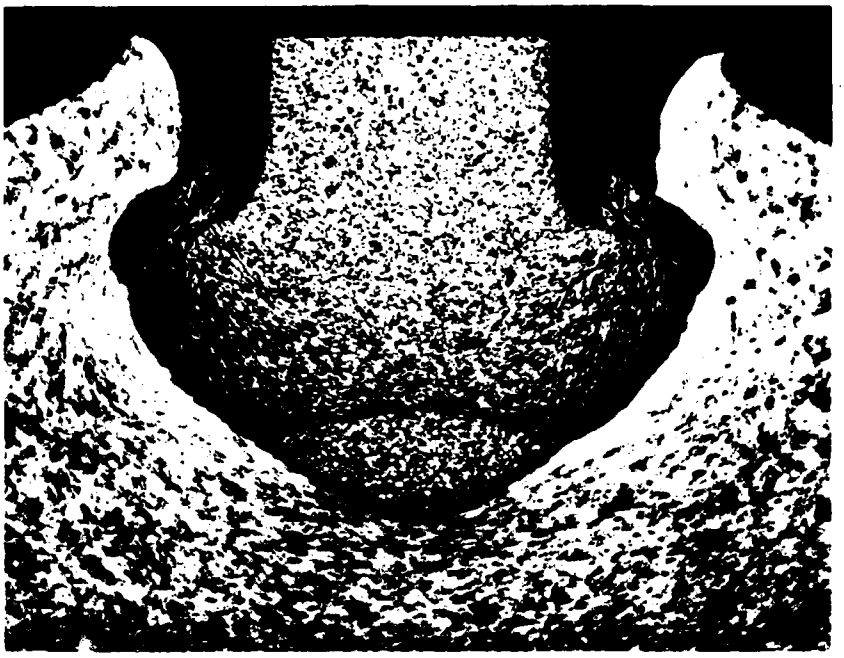

FIGURE 8 Cross section of a tungsten alloy, Kennertium W2, penetrator with 90° included angle conical end, which has been fired into an armour steel at 695 ms^{-1}. Note the stability of the nose of the penetrator and the large strains further back along the length of the penetrator.

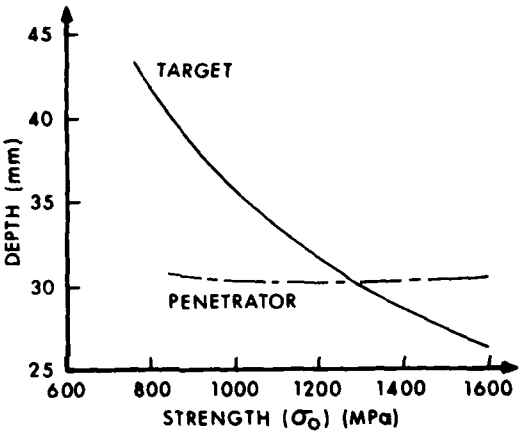

FIGURE 9 Influence of penetrator and target strength on depth of penetration of a tungsten round into a semi-infinite armour steel target. The basic material properties and geometric conditions used for the calculations are indicated in the text.

(MRL-R-811)

DISTRIBUTION LIST

MATERIALS RESEARCH LABORATORIES

Chief Superintendent
Superintendent, Metallurgy Division
Dr. M.E. de Morton
Library
R.L. Woodward
Librarian, Materials Testing Laboratories, NSW Branch

DEPARTMENT OF DEFENCE

Chief Defence Scientist
Deputy Chief Defence Scientist
Controller, Projects and Analytical Studies
Superintendent, Science and Technology Programmes
Controller Service Laboratories and Trials
Army Scientific Adviser
Air Force Scientific Adviser
Navy Scientific Adviser
Chief Superintendent, Aeronautical Research Laboratories
Chief Superintendent, Weapons Systems Research Laboratory
Chief Superintendent, Electronics Research Laboratory
Chief Superintendent, Advanced Engineering Laboratory
Superintendent, Trials Resources Laboratory
Senior Librarian, Defence Research Centre
Librarian, R.A.N. Research Laboratory
Officer-in-Charge, Document Exchange Centre (17 copies)
Technical Reports Centre, Defence Central Library
Central Office, Directorate of Quality Assurance - Air Force
Deputy Director Scientific and Technical Intelligence, JIO
Head, Engineering Development Establishment
Director of Naval Ordnance Inspection
Deputy Inspector of Naval Ordnance
Director of Operational Requirements (Air Office)
HQ Log. Command (QA Div.)
Librarian, Bridges Library, Royal Military College, Duntroon
Officer-in-Charge, Joint Tropical Trials and Research Establishment

DEPARTMENT OF INDUSTRY AND COMMERCE

NASA Canberra Office
Head of Staff, British Defence Research and Supply Staff (Aust.)
Controller, Munitions Supply Division
First Assistant Controller, Munitions Supply Division
Controller, Aircraft, Guided Weapons & Electronics Supply Division
Manager, Ordnance Factory, Bendigo
Manager, Ordnance Factory, Maribyrnong
Manager, Explosives Factory, Maribyrnong
Manager, Explosives Factory, Albion
Manager, Explosives Factory, Mulwala

DISTRIBUTION LIST
(Continued)

DEPARTMENT OF INDUSTRY AND COMMERCE

Manager, Ammunition Factory, Footscray
Manager, Small Arms Factory, Lithgow
Manager, Government Aircraft Factory, Port Melbourne

OTHER FEDERAL AND STATE DEPARTMENTS AND INSTRUMENTALITIES

The Chief Librarian, Central Library, CSIRO
Australian Atomic Energy Commission Research Establishment
(Attention: Library)
Chief, Division of Mechanical Engineering, CSIRO
(Attention: Librarian)
Chief, Production Technology Laboratory, CSIRO
(Attention: Librarian)

MISCELLANEOUS - OVERSEAS

Defence Scientific & Technical Representative, Australian High Commission, London, England
Assistant Director/Armour and Materials, Military Vehicles and Engineering Establishment, Surrey, England
Reports Centre, Directorate of Materials Aviation, Kent, England
Library - Exchange Desk, National Bureau of Standards, Washington, USA
US Army Standardization Representative, Canberra
The Director, Defence Scientific Information & Documentation Centre, Delhi, India
Colonel B.C. Joshi, Military, Naval and Air Adviser, High Commission of India, ACT
Director, Defence Research Centre, Kuala Lumpur
Overseas Reports Section, Defence Research Information Centre, Kent, England
Counsellor Defence Science, Embassy of Australia, Washington, USA
(Attention: Mr. R. Cummins)
Director, Royal Armament Research & Development Establishment, Fort Halstead, Kent, England (2 copies - 1 copy for attention of Mr. C. Oxlee)
Director General, Defence Research Establishment Valcartier, Canada. (2 copies - 1 copy for attention of Mr. W.J. Robertson, Armament Div.)
DRDAR-BLT, US Army Ballistics Research Laboratory, USA
(3 copies - Attention: Dr. J.A. Zukas
Mr. K. Frank
Mrs. B. Ringers